THE JOURNAL OF PHYSICAL CHEMISTRY C

Article

pubs.acs.org/JPCC

Trends in the Adsorption and Dissociation of Water Clusters on Flat and Stepped Metallic Surfaces

Rengin Peköz,*[,†] Svenja Wörner,[†,‡] Luca M. Ghiringhelli,[§] and Davide Donadio[†]

[†]Max Planck Institut für Polymerforschung, Ackermannweg 10, D-55128 Mainz, Germany

[‡]Fakultät für Chemie und Geowissenschaften, Ruprecht-Karls-Universität, Im Neuenheimer Feld 234, 69120 Heidelberg, Germany

[§]Fritz Haber Institute of the Max Planck Society, Faradayweg 4-6, D-14195 Berlin-Dahlem, Germany

Supporting Information

ABSTRACT: Understanding the structure and chemical reactivity of water adsorbed at metallic surfaces is very important in many processes such as catalysis, corrosion, and electrochemistry. Using density functional theory calculations, we investigate the adsorption and dissociation of water clusters on flat and stepped surfaces of several transition metals: Rh, Ir, Pd, and Pt. We find that water binds preferentially to the step edges than to terrace sites, thus linear clusters or one-dimensional water wires can be isolated by differential desorption. The clusters formed at the step are stabilized by the cooperative effect of chemical bonds with the metal and hydrogen bonding. The enhanced reactivity of the step edges and the cooperative effect of hydrogen bonding improve the chances of partial dissociation of water clusters. We assess the correlations between adsorption and dissociation energies, observing that they are increased on stepped surfaces. We present a detailed interpretation of water dissociation by analyzing changes in the electronic structure of both water and metals. The identification of trends in the energetics of water dissociation at transition metals is expected to aid the design of better materials for catalysis and fuel cells, where the density of steps at surfaces would be a relevant additional parameter.

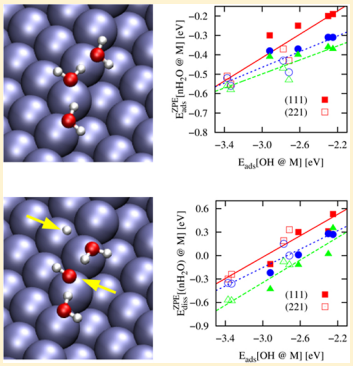

1. INTRODUCTION

The interaction of water with transition metal surfaces plays a fundamental role in several chemical processes such as catalytic surface reactions, corrosion, fuel cells, and hydrogen production.[1,2] These processes often include the formation and/or dissociation of water on metallic substrates. The adsorption of water on metal surfaces, often considered as a prototype system to understand more complicated water−solid interfaces, has been extensively investigated both experimentally and theoretically.[3−6] With the help of scanning probe microscopy and theoretical calculations, mostly at the level of density functional theory (DFT), it has been possible to get local images and to characterize the adsorption of water on metals.[7−9] These scanning probe techniques are mostly viable for well-defined low-index surfaces of single crystals, at low temperature, low coverage, and ultrahigh vacuum conditions. Changes in coverage and thermodynamic conditions result in water structures with different dimensionality, ranging from isolated monomers to one-dimensional (1D) chains, 2D layers, and 3D structures.[9−14] In addition, it is difficult to assess the protonation state of interfacial water by scanning probe microscopy, so that understanding the water−metal interfaces at the atomistic level remains a challenging open problem.

The effect of surface structure on catalytic reactions plays an important role to design efficient catalysts.[15−17] Although the adsorption of water on flat and defect-free surfaces has been extensively studied, the chemistry of water at high-index vicinal surfaces, occurring in realistic situations, is largely unexplored. Only recently, under the motivation of experimental findings,[7,10,18−20] theoretical studies have started to examine defect sites, such as steps and kinks, on the adsorption of water.[21−28] The contribution of surface defects to adsorption and dissociation energies is significant because these sites are usually more reactive than closed-packed surfaces. For example, the presence of steps and kinks is known to reduce the reaction barriers for water dissociation and hydrogen recombination on Cu surfaces.[15]

Considering the large number of potentially interesting systems for different applications and that both experiments and theoretical calculations are feasible for a limited number of systems, it is crucial to identify trends that may aid the search for materials with targeted functionalities.[29] So-called "scaling relations",[30] which correlate different adsorption energies, have been used to demonstrate trends in catalytic systems. For example, using the adsorption energies of C, N, O, and S on stepped and close-packed metal surfaces,[30,31] and OH on oxide surfaces,[32] the potential energy diagram for a surface catalyzed reaction was estimated. Other studies showed that the binding energy of methyl on metal surfaces[33,34] can be used as a descriptor for a DFT-based catalyst design.

In this paper, we investigate the adsorption and dissociation energies and geometries of small water clusters, from

Received: October 10, 2014
Revised: November 21, 2014
Published: November 24, 2014

monomers to trimers, on close-packed (111) and higher-index (211) surfaces of rhodium, iridium, palladium, and platinum, by means of DFT calculations, including nuclear quantum effects in the form of zero-point energy (ZPE) corrections, evaluated within the quantum harmonic-oscillator approximation. The trends among different adsorption energies and adsorption and dissociation energies are analyzed to obtain a general understanding of water activity on flat (111) and stepped (221) transition metal surfaces. We examine the cooperative effect of hydrogen bonding (HB) between water molecules and surface bonding, which stabilizes the adsorption and dissociation states on both surfaces. This analysis reveals that the increased reactivity of atoms at the edge of steps enhances the adsorption energies of intact clusters. Moreover, the cooperative effect of hydrogen bonding increases the chance of partial dissociation of water clusters at steps. In addition to the scaling relations between different adsorption energies, we also show that the dissociation energies of water clusters on metallic surfaces correlate positively with the adsorption energies.

2. METHODS

First-principles total energy calculations within the density functional theory were performed to investigate the adsorption and dissociation properties of water clusters (monomer to trimer) on (111) and (221) surfaces of Rh, Ir, Pt, and Pd. Ultrasoft pseusopotentials (USPP)[35] were used to describe the interactions between ions and electrons. A plane wave basis set with a cutoff energy of 35 (for Rh and Pt), 40 (for Ir), and 45 (for Pd) Ry was employed. We applied the exchange and correlation functional by Perdew, Burke, and Ernzerhof (PBE).[36] The integration over the first Brillouin zone was performed using Monkhorst−Pack[37] k-point meshes of $4 \times 3 \times 1$ for the (221) slabs with 4×1 periodicities and similar meshes of $4 \times 4 \times 1$ were used for (111) slabs and (221) slabs with 3×1 periodicities. The Methfessel−Paxton approach[38] with a Gaussian broadening of 0.27 eV was used to smear the electronic occupation at the Fermi level. The convergence threshold on forces for ionic relaxations was set to 10^{-3} atomic units (au). Several tests have been performed to verify the convergence of results.[39] The calculations were carried out using the Quantum-ESPRESSO package.[40]

The chosen PBE functional has proven good accuracy in describing H-bonding in ice[41] as well as the structure and energetics of small water clusters.[42−44] The adsorption energies of water monomers on flat Pd and Pt surfaces are instead systematically underestimated compared to experiments (0.25 vs 0.45 eV),[45,46] and no experimental data is available for Rh and Ir. Considering explicitly van der Waals (vdW) interactions would substantially contribute to the adsorption energies of water on metals. However, it was recently shown that accounting for dispersion forces would not change either relative binding energies or adsorption geometries and therefore would not affect the observed trends.[47]

The calculated lattice constants of bulk Pd, Pt, Ir, and Rh are 3.98, 4.01, 3.89, and 3.86 Å, respectively: all within 1.5−2.3% of the experimental value of 3.89, 3.92, 3.84, and 3.80 Å, respectively.[48,49] The supercells used for the (111) surfaces were $(4 \times 2\sqrt{3})$ for all calculations with a total of 48 metal atoms. The stepped (221) surfaces were cut from bulk metal supercells with the terraces having a (111) orientation and the monatomic (110) steps are separated by four atomic rows. p(3x1) supercells (42 metal atoms) were used to study monomers and dimers on stepped surfaces, while larger supercells, p(4x1) (56 metal atoms) were used for trimers. The surfaces were modeled by four layers of metals, and the vacuum space was set to 20 Å. The two bottom layers were fixed, and the rest of the system was relaxed.

The ZPE of the vibrational modes induces significant shifts in both binding and dissociation energies:[26,50,51] for example, the inclusion of ZPE correction has been shown to decrease the adsorption energy of water clusters on flat and stepped Pt surfaces by ∼0.1 eV.[21,50] Thus, we computed the vibrational frequencies of the adsorbed and dissociated systems to take into account quantum effects in terms of ZPE. The vibrational analysis is carried out using the frozen phonon approach, in which the force constant matrix of the adsorbate is computed by finite differences of the forces. We use a finite displacement of the atoms of 0.01 Å. The ZPE corrections to the adsorption and dissociation energies are expressed as $\Delta E_{ZPE} = \sum_i \hbar\Delta\omega_i/2$, where the sum runs over the vibrational modes of the molecules adsorbed on the surface. $\Delta\omega$ indicates the difference between the vibrational frequencies either of water in gas phase and adsorbed at the surface or of intact and dissociated adsorbates. All reported adsorption and dissociation energies take into account the ZPE correction, unless otherwise noted.

The adsorption energy (E_{ads}) per water molecule is calculated as

$$E_{ads} = (E[(H_2O)_n@M] - n\cdot E[H_2O] - E[M])/n \quad (1)$$

where n is the number of water molecules in the simulation cell, $E[(H_2O)_n@M]$ is the total energy of the metal surface (M) with the adsorbed molecule, $E[H_2O]$ is the energy of a single water molecule in gas phase, and $E[M]$ is the energy of the bare metal surface. Consequently, a negative adsorption energy means energetically favored adsorption.

The dissociation energy, E_{diss}, is calculated as the total energy difference between the dissociated structure and the intact one, such as

$$E_{diss} = E[((H_2O)_{(n-1)} + OH^- + H^+)@M] - E[(H_2O)_n@M] \quad (2)$$

where negative E_{diss} indicates exothermic dissociation.

We tested the dissociation energy of water monomer on Ir surfaces with different exchange-correlation functionals (PBE, PBEsol,[52,53] and PW91[54]) and pseudopotentials (USPP, Troullier−Martins (TM),[55] and projector augmented wave (PAW)[56,57]). The E_{diss} calculated with different density functionals ranges from 0.23 to 0.47 eV for Ir(111) and −0.09 to −0.19 eV for Ir(221). For more details, see the Table S1 in Supporting Information (SI)).

3. RESULTS

In this section, we first present the adsorption and dissociation energetics and structure of water clusters, including monomers, dimers, and trimers, on (111) metal surfaces. The following part of this study is extended to (221) metal surfaces, and the adsorption and dissociation of clusters are explored. The electronic structure calculations are discussed in section 3.5. Then, the trends in the adsorption and dissociation energies of water clusters on different metals and surface types are discussed in section 4.

3.1. Adsorption of Water Clusters on (111) Surfaces.

We have first investigated the adsorption of a water monomer on flat Rh, Ir, Pt, and Pd surfaces. We have found that the most favorable adsorption site with the PBE functional is atop

dx.doi.org/10.1021/jp510242h | J. Phys. Chem. C 2014, 118, 29990−29998

(Figure 1a), consistent with previous studies.[5,21,58−61] The plane containing the dipoles of monomers adsorbed on (111)

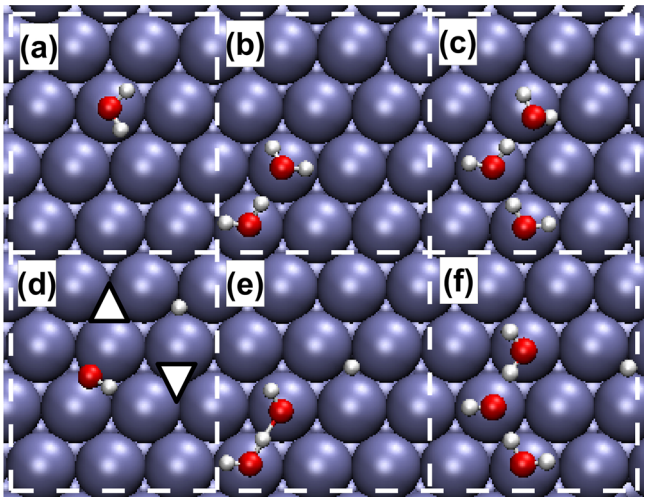

Figure 1. Relaxed geometries of intact and dissociated water (a and d) monomer, (b and e) dimer, and (c and f) trimer on Rh(111) surface. The periodically replicated cells used in the calculations are represented by white dashed lines. The fcc- and hcp-hollow sites are represented in (d) by the triangles pointing up and down, respectively. The dissociated proton always sits on a fcc-hollow site.

surfaces is tilted with respect to the surface because of the directional interaction of $1b_1$ molecular orbital of water with the metal. The adsorption energies of water monomers on flat surfaces are summarized in Table 1. The interaction of water

Table 1. Calculated Adsorption Energy per Water Molecule with (E_{ads}^{ZPE}) and without (E_{ads}), and Dissociation Energies with (E_{diss}^{ZPE}) and without (E_{diss}) Zero-Point Energy Corrections for Water Clusters on (111) Surfaces[a]

surface	cluster	E_{ads} [eV/H_2O]	E_{ads}^{ZPE} [eV/H_2O]	E_{diss} [eV]	E_{diss}^{ZPE} [eV]
Rh(111)	$1H_2O$	−0.36	−0.30	0.05	−0.11
	$2H_2O$	−0.46	−0.38	−0.03	−0.22
	$3H_2O$	−0.49 (−0.46)	−0.41	−0.29	−0.43
Ir(111)	$1H_2O$	−0.32	−0.25	0.47	0.30
	$2H_2O$	−0.45	−0.37	0.20	0.01
	$3H_2O$	−0.47 (−0.43)	−0.40	0.01	−0.12
Pt(111)	$1H_2O$	−0.25	−0.20	0.70	0.53
	$2H_2O$	−0.39	−0.31	0.47	0.27
	$3H_2O$	−0.43 (−0.28)	−0.37	0.37	0.24
Pd(111)	$1H_2O$	−0.25	−0.20	0.46	0.31
	$2H_2O$	−0.38	−0.31	0.44	0.28
	$3H_2O$	−0.41 (−0.40)	−0.36	0.20	0.02

[a]The adsorption energies of ring-like configurations are presented in parentheses for trimers.

monomers with Rh and Ir is stronger than that with Pt and Pd, yielding a stability order Rh > Ir > Pt > Pd. Even though the present computational framework is different, the results are in good agreement with those of several previous studies[21,47,50,59−64] (SI, Table S2). The details of the optimized structural parameters are collected in SI, Table S3.

The water dimer on metal surfaces is the simplest H-bonded water system on surfaces. Because H-bonding between water molecules and water−metal interaction takes place at the same time, water dimers on metallic substrates reveal important information on the cooperative effect of these two interactions. As shown in Figure 1b, both proton donor (D) and acceptor (A) [the molecule donating its hydrogen atom in the H-bond is called "donor", and the other one accepting the hydrogen atom in the H-bond is called "acceptor"] prefer atop sites on all the surfaces considered. On the other hand, the O−metal distance is very different for the H-bond donor (2.22−2.30 Å) with respect to the acceptor (3.01−3.20 Å), indicating much weaker surface water interaction for the latter. Compared to their gas-phase counterparts, the distance between the oxygen atoms of the adsorbed dimer significantly decreases by 0.18 Å and the O−H bond length of donor increases slightly by 0.02 Å, pointing out that the H-bonding in adsorbed dimer is enhanced. The reason is that the dipole moment of the donor is increased by polarization effects induced by the metal surface.[14]

The presence of a second water molecule, resulting in the formation of a H-bond between adsorbed molecules, increases the adsorption energy per molecule by about 0.13 eV compared to the monomer (see Table 1). The stability order is the same as for the monomer case, with the adsorption energies ranging from −0.38 (for Rh) to −0.31 eV (for Pd). The cooperative effect between the H-bonding and O−metal bonding can be better understood by separating the adsorption energy into hydrogen bonding (E^{ww}) and O−metal interactions (see section 4 in SI, Table S4). The contribution of hydrogen bonding to the adsorption energy per water molecule goes from 53 to 78 meV, and as the clusters increase in size E^{ww} increases.

Further increasing the number of water molecules results in different possible configurations with competing binding energies. For example, Meng et al.[59] claimed that trimer adsorbed on Pt(111) surface would retain a ring-like geometry with one OH contributing to the H-bonding and the other free for each water molecules so each of them behave as donor−acceptor. Thus, we have investigated two different adsorption configurations, ring- and chain-like, on the metal surfaces (see SI, Figure S1). We have found that the chain-like structure is slightly more favorable, as the system prefers to form linear hydrogen bonds than very distorted ones, as in the case of rings. In addition, the chain-like structure favors stronger water−metal interactions, especially for the H-bond donor (see SI, Table S5).

The adsorption energy of trimers increases by 0.03 eV/H_2O compared to dimers. This small energy gain can be explained by the increased number of H-bonds formed between water molecules, which is partly compensated by the weaker H-bond formed between the acceptor/surface and central/surface. The O−metal and H-bond contributions to the adsorption energy of each system are summarized in SI, Table S3. The adsorption order is the same as for the monomer and dimer cases, with the adsorption energy ranging from −0.41 (for Rh) to −0.36 eV (for Pd).

3.2. Adsorption of Water Clusters on (221) Surfaces.

The adsorption energies of monomers on stepped surfaces are significantly larger than those on flat surfaces, by 0.17−0.30 eV, in good agreement with the previous calculations,[21,65] due to the increased reactivity of step edges (see Table 2). Water monomers prefer to sit at atop sites at the step edge rather than at kinks or on terraces (see Figure 2a). The distance between

dx.doi.org/10.1021/jp510242h | J. Phys. Chem. C 2014, 118, 29990−29998

Table 2. Calculated Adsorption Energy per Water Molecule with (E_{ads}^{ZPE}) and without (E_{ads}) and Dissociation Energies with (E_{diss}^{ZPE}) and without (E_{diss}) Zero-Point Energy Corrections for Water Clusters on (221) Surfaces

surface	cluster	E_{ads} [eV/H_2O]	E_{ads}^{ZPE} [eV/H_2O]	E_{diss} [eV]	E_{diss}^{ZPE} [eV]
Rh(221)	$1H_2O$	−0.57	−0.51	−0.14	−0.30
	$2H_2O$	−0.58	−0.52	−0.19	−0.35
	$3H_2O$	−0.63	−0.56	−0.45	−0.57
Ir(221)	$1H_2O$	−0.62	−0.55	−0.09	−0.24
	$2H_2O$	−0.63	−0.56	−0.18	−0.36
	$3H_2O$	−0.65	−0.58	−0.48	−0.60
Pt(221)	$1H_2O$	−0.48	−0.43	0.51	0.33
	$2H_2O$	−0.55	−0.49	0.20	0.00
	$3H_2O$	−0.57	−0.53	0.01	−0.12
Pd(221)	$1H_2O$	−0.43	−0.37	0.34	0.19
	$2H_2O$	−0.49	−0.43	0.29	0.15
	$3H_2O$	−0.53	−0.47	0.03	−0.08

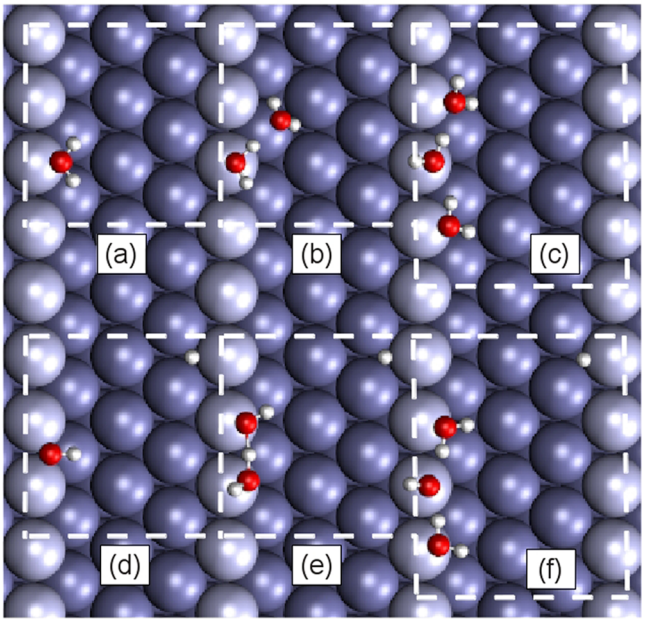

Figure 2. Relaxed geometries of intact and dissociated water (a and d) monomer, (b and e) dimer, and (c and f) trimer on Rh(221) surface. The step-edge atoms are shown with lighter color. The periodically replicated cells used in the calculations are represented by white dashed lines.

the O atom and the closest metal atom ranges from 2.27 (for Rh) to 2.35 Å (for Pd), and H atoms are tilted toward the lower terrace. The O−metal distances are shorter than those of flat surfaces by 0.06 Å, indicating stronger chemical bonding.

While a good matching of hydrogen bonding distance to the nearest neighbor distance of the metal atoms of the step edge (2.8 Å) may facilitate adsorption, in the case of dimers, only the HB donor binds strongly to the metal. The HB acceptor sits farther from the step edge and forms a weak H-bond with the lower terrace of the metals (see Figure 2b). H-Bonding makes the binding of dimers only slightly stronger than that of monomers. These small energies gained for dimers, 0.01 eV for Rh and Ir, and 0.06 eV for Pt and Pd compared to monomers, can be explained by analyzing their relaxed geometries in detail. The oxygen atom of the H-bond donor is bonded to the step atoms of Rh and Ir (Pt and Pd) with O−metal distances of 2.19(2.23) Å, whereas the acceptor is farther from the step with O−metal distances of 3.62(3.38) Å (SI, Table S6). The interaction between H-bond acceptor and the step atoms of group 9 elements significantly weakens compared to that for group 10 elements, thus the energy gained by the formation of a H-bond between molecules is compensated by the weaker O−metal interaction.

The addition of another water molecule causes further increase in the adsorption energies with respect to dimers. These small energies gained in trimers are the result of increasing the number of H-bonds in clusters, which are partly compensated by a weaker attraction between the molecules and the metal. The adsorbed configurations of trimers on metal stepped surfaces display two of the water molecules (donor and central) bonded atop on the step edges and a H-bond acceptor detached from the step (Figure 2c). The hydrogen atoms of the attached molecules are in alternating directions, and one of the hydrogen atoms of the acceptor points toward the lower terrace. The calculated equilibrium O−metal distances and other geometrical details are presented in SI, Table S6. Other possible trimer configurations on Pt(221) were suggested,[21,26] however, these row-like configurations are less stable by 0.08 eV than the one proposed here (see SI, Table S5 and Figure S1e).

3.3. Dissociation of Water Clusters on (111) Surfaces.

We have investigated the dissociation of one water molecule for each nH_2O cluster, with the resulting intermediates being $H^+ + OH^- + (n-1)H_2O$ on metal surfaces. The calculated adsorption sites for the dissociation of water monomers are in agreement with those suggested for OH adsorption in former theoretical studies.[50,62,63] The hydroxyl is adsorbed on a bridge site for all metals (see Figure 1d for a monomer dissociation on a metal surface), while the dissociated proton sits on an fcc-hollow site.[64] Further details on the structural parameters of the dissociation are reported in SI, Table S7.

The dissociation energies with (E_{diss}^{ZPE}) and without (E_{diss}) ZPE correction are collected in Table 1 and shown in Figure 3.

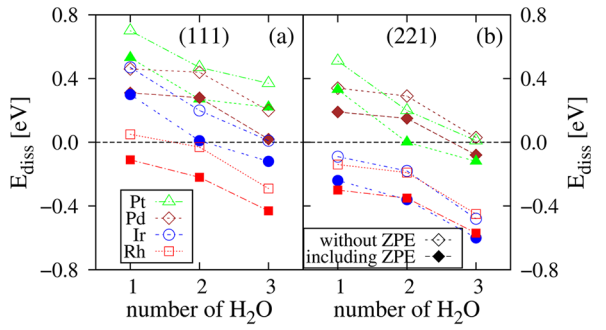

Figure 3. Dissociation energies of water clusters for (a) (111) and (b) (221) surfaces. In both panels, full symbols (open symbols) mark dissociation energies including (without) zero-point energy correction.

The E_{diss} on flat Pt, Ir, and Rh surfaces are in good agreement with the previously reported dissociation energies.[50,61] Small differences with respect to former studies arise (about 0.07 eV) due to the different simulation setup chosen, among which are coverage, exchange correlation functional, and pseudopoten-

dx.doi.org/10.1021/jp510242h | J. Phys. Chem. C 2014, 118, 29990−29998

tials. ZPE correction stabilizes E_{diss} by 0.15−0.17 eV and leads to exothermic dissociation on Rh surface.

Because of the adsorption configurations of water dimers and trimers, discussed in the previous section, the hydrogen of the HB acceptor pointing toward the metal surface offers the easiest path for partial dissociation. The dissociated dimer and trimer configurations are presented in parts e and f of Figure 1, respectively. Because of the structural rearrangements between O−O and O−metal, breaking an O−H bond costs less energy than splitting monomers. For example, E_{diss}^{ZPE} of the dimer decreases by 0.29 eV for Ir(111) with respect to the monomer and is nearly iso-energetic (E_{diss}^{ZPE} = 0.01 eV) (see Table 1). Upon splitting of a water molecule, the OH^--H_2O interaction gets stronger with O−O bond length, decreasing by 0.22 Å for dimers compared to the intact dimer cases.

In the case of trimer, breaking the O−H bond of the HB acceptor results in a proton transfer mechanism, which leads to a stable configuration (Figure 1f). The remaining OH^- is the central molecule of the cluster which accepts hydrogen bonds from both neighboring water molecules. The water−metal interaction and hydrogen bonding between water molecules are stronger in the dissociated geometries. These tighter interactions cooperate to compensate the energy loss from splitting the O−H covalent bond, thus making dissociation possible. Moreover, ZPE correction stabilizes further dissociated species on surfaces. For instance, the partial dissociation of trimer turns from iso-energetic to exothermic on Ir surface and from endothermic to almost iso-energetic on Pd surface.

3.4. Dissociation of Water Clusters on (221) Surfaces. The products of the dissociation of a water monomer, OH^- and H^+, adsorb on bridge position at the step edge and on hollow terrace site, respectively. When a water monomer is dissociated on a (221) surface, the OH^- adsorbs on bridge position at the step edge and the H^+ adsorbs on the terrace. The distance between the hydroxyl and the closest step atom is about 2.1 Å. The structural parameters are given in SI, Table S8. The most favorable adsorption site for the dissociated proton was previously investigated for Pt(221), and it was reported that the fcc-hollow site adjacent to the step edge was energetically the most favorable.[26] We explored the adsorption energy of an atomic hydrogen on Rh(221) surface by taking into account different adsorption sites, and we found that the preferred adsorption site is again the fcc-hollow (see SI, Table S9). Thus, we assume that the same proton adsorption site holds also for Pd and Ir stepped surfaces.

The increased reactivity of the metal atoms at the step edge facilitates the dissociation of water monomer compared to flat surfaces by 0.19 for Rh, 0.54 for Ir, 0.20 for Pt, and 0.12 eV for Pd (see Table 2). Similar to the case of flat surfaces, the dissociation of a monomer is endothermic on Pt and Pd stepped surfaces, while it turns from endothermic to exothermic on Ir and is exothermic on both flat and stepped Rh surfaces. The energy required to break a covalent O−H bond is partially compensated by the formation of a stronger O−metal bond: the balance between these two energetics decides on the character of dissociation.

In the dimer, the H-down molecule, already detached from the step edge, facilitates its partial dissociation. The optimal configurations with oxygen atoms bonded to atoms at the step edge and the geometry of dissociated dimer on (221) surface is presented in Figure 2e. The distances between the oxygen atoms are reduced by ∼0.2 Å compared to the intact dimers, showing that stronger chemical bonds are formed not only between the hydroxyl and step edge atoms but also between the hydroxyl and the neighboring water molecules. The energy required to break an O−H bond is compensated by the formation of new OH−metal bond, the adsorption of proton, and by a stronger H-bond between water and hydroxyl. The dissociation of water dimers is exothermic on Rh(221) and Ir(221), iso-energetic on Pt(221), and endothermic on Pd(221) yet with a reduced energy cost.

The dissociation of one water molecule in trimers takes place in a similar way to dimers, i.e., the detached H-bond acceptor releases the H atom initially pointing toward the lower terrace and adsorbed on the lower terrace. The interesting part in the dissociation process is the proton transfer occurring within the clusters. The relaxed geometry, displayed in Figure 2f, shows that the central water molecule is responsible for the proton transfer mechanism by giving its H atom to the dissociated one and accepting hydrogen bonds from the neighboring molecules. The distances among neighboring water molecules and with the step edge atoms are smaller than the intact trimer. This leads to the conclusion that water−water and water−metal interactions are stronger than those for intact trimers. The partially dissociated configurations of water on group 9 and group 10 stepped surfaces are energetically more favorable than their intact geometries by about 0.58 and 0.10 eV, respectively.

3.5. Projected Density of States. To shed light on the bonding between water clusters and metal surfaces, we have calculated the density of states (DOS) of the molecules and surfaces. The surfaces of Rh and Ir show a much higher DOS distribution near the Fermi level than those of Pt and Pd, which makes them more reactive. The empty(filled) electronic states near the Fermi level can accept(donate) more electrons to enhance the reduction(oxidation) reactions.

The DOS projected on the atomic orbitals of the oxygen *p*-states and *d*-states of the (upper layer) metal atoms onto which OH and/or H_2O is adsorbed are computed for both intact and dissociated clusters on flat and stepped surfaces. Because the general behavior is similar among the different metals considered here, only the projected DOS (pDOS) for Ir(111) and Ir(221) surfaces are shown in Figure 4 and the pDOS of the other systems are displayed in SI, Figures S3−S6. The deep $2a_1$ and $1b_2$ molecular orbitals of water lie far below the Fermi level (about 22 and 10 eV, respectively), and thus they interact very weakly with the metal states and are not shown in the pDOS. The $1b_1$ and $3a_1$ states are shifted down in energy with respect to their free molecular states and the $1b_1$ state hybridizes with the *d*-states of the substrates showing covalent bond behavior.

The oxygen-related *p*-states of all the intact clusters are well localized. For the donor molecule, which is closer to the surface than the acceptor and the central molecule, the O *p*-states are broadened. On the stepped surfaces, because the adsorption is stronger, the O *p*-states of the donor molecules are more broadened than those on flat surfaces. There is no significant difference between the *p*-state of the acceptor molecule of dimer on flat and stepped surfaces because their adsorption geometries are similar on both surfaces. On the other hand, the O *p*-states of the central molecule in trimers differ significantly between flat and stepped surfaces. On the flat surface, the bonding between the central molecule and the surface is as weak as it is for the acceptor molecule, while on the step edge the central molecule is closer to the surface and has a stronger interaction with the step edge atoms, leading to more broadening. Dissociation leads to significant distortions of the

dx.doi.org/10.1021/jp510242h | J. Phys. Chem. C 2014, 118, 29990−29998

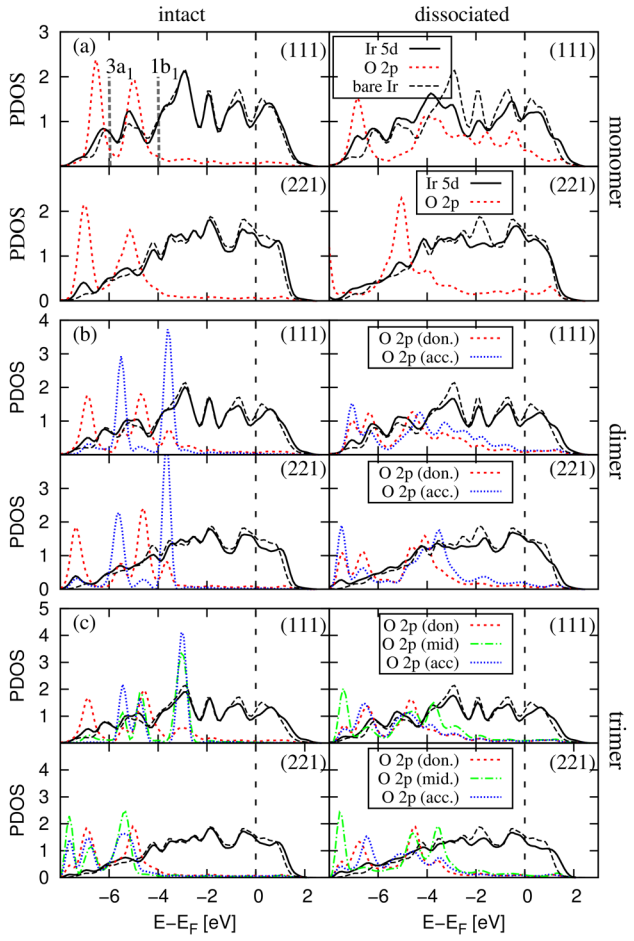

Figure 4. pDOS of O *p*-states and *d*-states of the Ir atoms onto which OH^- and/or H_2O is adsorbed on the surface for the (a) monomer, (b) dimer, and (c) trimer adsorbed on flat and stepped Ir surfaces. Left and right panels correspond to intact and dissociated configurations, respectively. The Fermi level is set to 0 eV. The dashed gray lines in (a) represent the $1b_1$ and $3a_1$ water orbitals in the gas phase, and the energy levels of water in vacuum have been shifted so that $2a_1$ levels of water in gas and on Ir coincide.

O *p*-states, and a strong hybridization between the molecular and surface states takes place. All of the *p*-states are broadened and hybridize with the *d*-states of the metal.

4. DISCUSSION

From the collection of data presented above, we can now identify trends that may contribute to the general understanding of the chemistry of water at transition metal surfaces. Both the adsorption and the dissociation of water clusters are related to the reactivity of the metallic surfaces. We then argue that there can be a relation between adsorption and partial dissociation energies of water clusters on flat and stepped surfaces (Figure 5). Atoms at steps have different coordination, which leads to different electronic properties. The electron density at low coordinated step edges is smoothed, i.e., electrons move from step edge toward the lower terrace so that their kinetic energy is lowered.[66] This smoothing induces a charge dipole that interacts with the local charges of adsorbed molecules, thus increasing the reactivity of the steps. The higher reactivity at step sites not only enhances the adsorption energy of water clusters but it also facilitates their partial dissociation. The stepped surfaces augment the adsorption energy of water

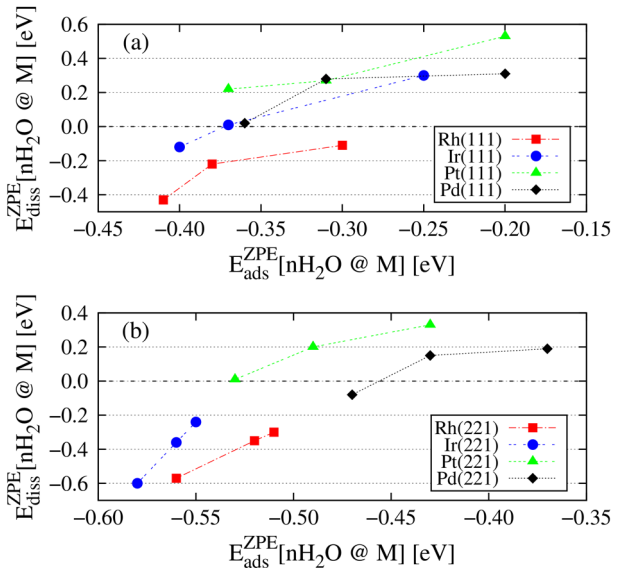

Figure 5. Adsorption vs dissociation energies of water clusters on (a) (111) and (b) (221) surfaces. The right most and left most points represent monomers and trimers, respectively, for each metal.

clusters by 0.11−0.23 eV and favor dissociation by 0.10−0.54 eV. While flat surfaces show a single trend on the adsorption versus dissociation energies, the elements of period V and VI for stepped surfaces display different trends due to the enhanced atomic character of the low-coordinated step atoms (see Figure 5).

The scaling relations, also known as "corollary d-band model", relate the adsorption energy of any hydrogen containing molecule, AH_x, with the adsorption energy of its heavy atom, *A*.[30] Because the adsorption energies of O and OH are strongly correlated,[67] the scaling relation holds between the adsorption energy of OH[65,68−72] and adsorption and dissociation of water clusters. Here we probe the scaling relations for the adsorption of water clusters and we extend them, showing that also the dissociation energies correlate linearly with the adsorption energy of hydroxyl.[73]

Figure 6 illustrates the scaling relations of the adsorption and dissociation energies of nH_2O with the adsorption energy of OH. In general, the scaling behavior of each data set (from monomer to trimer) has very similar linear relations for adsorption and dissociation energies. The scatter around the linear relations can be attributed to the differences in surface geometries and thus leading to different adsorption energies. For instance, the adsorption energy of hydroxyl on different metals varies by 0.5 eV from flat to stepped surfaces. Figure 6a shows that increasing the number of water molecules does not have a significant effect on the scaling relations, with slopes very close to each other, for different surface geometries (see SI, Figure S2). The adsorption energy of hydroxyl, which is an indicator of the energetics of the dissociation of water, enhances the differences in reactivity of stepped surfaces between group 9 and 10 elements. This analysis shows that the propensity of water clusters to dissociate is mostly determined by the adsorption energy of the single hydroxyl and that hydrogen bonding contributes to stabilize the dissociated phase with a nearly rigid shift toward lower energies of the E_{diss}^{ZPE} vs E_{ads} linear fit.

dx.doi.org/10.1021/jp510242h | J. Phys. Chem. C 2014, 118, 29990−29998

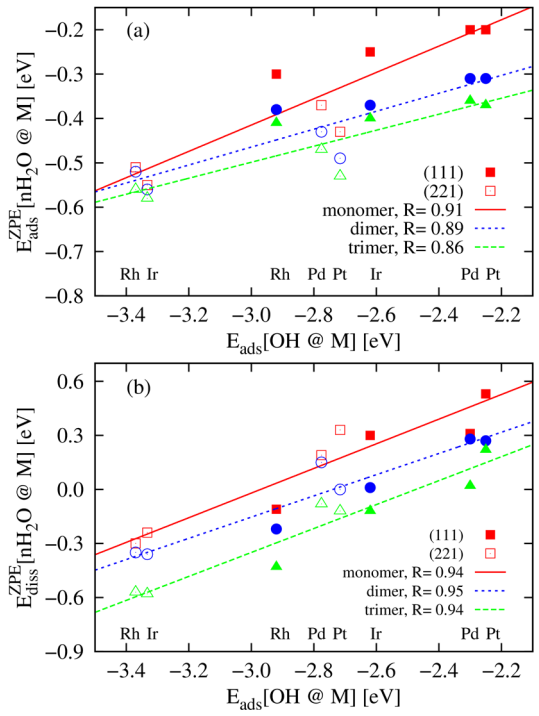

Figure 6. Scaling relations for nH_2O with n = 1 (square, red), n = 2 (circle, blue), and n = 3 (triangle, green) among the adsorption energy of OH^- and (a) adsorption energies of water clusters and (b) dissociation energies of water clusters on flat (full symbols) and stepped (open symbols) surfaces. Pearson's correlation (R) is indicated in the legends.

5. CONCLUSION

In summary, the interaction of adsorbed and dissociated water clusters with flat and stepped metallic surfaces has been systematically investigated in detail by means of density functional theory calculations. Our results confirm that water molecules prefer to adsorb at the edge of steps rather than at terraces. The adsorption order of the water clusters on flat and stepped surfaces is found as Rh > Ir > Pt > Pd and Ir > Rh > Pt > Pd, respectively. Increasing the number of water clusters results in stronger adsorption due to H-bonding. The increased reactivity of low coordinated stepped surfaces and the cooperative effect of H-bonding facilitate the dissociation of water clusters on stepped surfaces. For instance, while only the water dimer and trimer could dissociate on Rh(111), the dissociation energy of all the clusters is exothermic on stepped Rh and Ir surfaces and dissociation of trimers on stepped Pt and Pd surfaces turns to almost iso-energetic. Quantum effects, accounted for as ZPE correction, favor dissociation and systematically shift E_{diss} by ∼0.2 eV.

Scaling relations, among the adsorption energy of hydroxyl and the adsorption and dissociation energy of water clusters, suggest that the adsorption energy of OH^- is what mainly determines the energetics of water splitting, followed by the cooperative effect of hydrogen bonds in stabilizing partially dissociated clusters. This effect is magnified at steps which also enhance the differences in reactivity between group 9 and group 10 transition metals.

The shift in the energetics of water dissociation at steps is expected to play a prominent role in catalysis and fuel cells reactions, as the density of steps at surfaces could be an additional parameter to design more efficient anode materials or catalytic substrates. We hope that the trends presented here will contribute to understand and develop specific types of catalysts and reactions.

■ ASSOCIATED CONTENT

Supporting Information

Geometrical details of adsorbed and dissociated water clusters on (111) and (221) metal surfaces. Water−water and water−metal interaction energies. Adsorption energies and sites of H on Rh(221). pDOS of the systems. This material is available free of charge via the Internet at http://pubs.acs.org.

■ AUTHOR INFORMATION

Corresponding Author

*Phone: +49 (0)6131 379245. E-mail: pekoez@mpip-mainz.mpg.de.

Notes

The authors declare no competing financial interest.

■ ACKNOWLEDGMENTS

We thank Matthias Scheffler and Robinson Cortes Huerto for a critical reading of the manuscript and valuable discussions. We acknowledge the provision of computational facilities and support by Rechenzentrum Garching of the Max Planck Society and access to the supercomputer JUQUEEN at the Jülich Supercomputing Centre under project HMZ33. R.P. and D.D. acknowledge funding from the MPRG program of the Max Planck Society. L.M.G. acknowledges the cluster of excellence "Unifying Concepts in Catalysis" (UniCat, sponsored by the DFG and administered by the TU Berlin) for financial support.

■ REFERENCES

(1) Khaselev, O.; Turner, J. A Monolithic Photovoltaic-Photoelectrochemical Device for Hydrogen Production via Water Splitting. *Science* **1998**, *280*, 425−427.

(2) Chen, Y. W.; Prange, J. D.; Dühnen, S.; Park, Y.; Gunji, M.; Chidsey, C. E. D.; McIntyre, P. C. Atomic Layer-Deposited Tunnel Oxide Stabilizes Silicon Photoanodes for Water Oxidation. *Nature Mater.* **2011**, *10*, 539−544.

(3) Henderson, M. A. The Interaction of Water with Solid Surfaces: Fundamental Aspects Revisited. *Surf. Sci. Rep.* **2002**, *46*, 1−308.

(4) Michaelides, A. Density Functional Theory Simulations of Water−Metal Interfaces: Waltzing Waters, a Novel 2D Ice Phase, and More. *Appl. Phys. A: Mater. Sci. Process.* **2006**, *85*, 415−425.

(5) Hodgson, A.; Haq, S. Water Adsorption and the Wetting of Metal Surfaces. *Surf. Sci. Rep.* **2009**, *64*, 381−451.

(6) Li, J.; Zhu, S.; Wang, F. Metals Supported Water Monomers: The Bonding Nature Revisited. *J. Mater. Sci. Technol.* **2010**, *26*, 97−105.

(7) Nakamura, M.; Sato, N.; Hoshi, N.; Soon, J. M.; Sakata, O. One-Dimensional Zigzag Chain of Water Formed on a Stepped Surface. *J. Phys. Chem. C* **2009**, *113*, 4538−4542.

(8) Schiros, T.; Andersson, K. J.; Pettersson, L. G. M.; Nilsson, A.; Ogasawara, H. Chemical Bonding of Water to Metal Surfaces Studied with Core-Level Spectroscopies. *J. Electron Spectrosc. Rel. Phenom.* **2010**, *177*, 85−98.

(9) Nie, S.; Feibelman, P. J.; Bartelt, N. C.; Thürmer, K. Pentagons and Heptagons in the First Water Layer on Pt(111). *Phys. Rev. Lett.* **2010**, *105*, 026102.

(10) Morgenstern, M.; Michely, T.; Comsa, G. Anisotropy in the Adsorption of H_2O at Low Coordination Sites on Pt(111). *Phys. Rev. Lett.* **1996**, *77*, 703.

(11) Cerda, J.; Michaelides, A.; Bocquet, M.-L.; Feibelman, P. J.; Mitsui, T.; Rose, M.; Fomin, E.; Salmeron, M. Novel Water Overlayer Growth on Pd(111) Characterized with Scanning Tunneling

Microscopy and Density Functional Theory. *Phys. Rev. Lett.* **2004**, *93*, 116101.
(12) Thürmer, K.; Bartelt, N. C. Nucleation-Limited Dewetting of Ice Films on Pt(111). *Phys. Rev. Lett.* **2008**, *100*, 186101.
(13) Salmeron, M.; Bluhm, H.; Tatarkhanov, M.; Ketteler, G.; Shimizu, T. K.; Mugarza, A.; Deng, X.; Herranz, T.; Yamamoto, S.; Nilsson, A. Water Growth on Metals and Oxides: Binding, Dissociation and Role of Hydroxyl Groups. *Faraday Discuss.* **2009**, *141*, 221−229.
(14) Carrasco, J.; Hodgson, A.; Michaelides, A. A Molecular Perspective of Water at Metal Interfaces. *Nature Mater.* **2012**, *11*, 667−674.
(15) Fajin, J. L. C.; Cordeiro, M. N. D. S.; Illas, F.; Gomes, J. R. B. Influence of Step Sites in the Molecular Mechanism of the Water Gas Shift Reaction Catalyzed by Copper. *J. Catal.* **2009**, *268*, 131−141.
(16) Hendriksen, B. L. M.; et al. The Role of Steps in Surface Catalysis and Reaction Oscillations. *Nature Chem.* **2010**, *2*, 730−734.
(17) Vang, R. T.; Honkala, K.; Dahl, S.; Vestergaard, E. K.; Schnadt, J.; Laegsgaard, E.; Clausen, B. S.; Norskov, J. K.; Besenbacher, F. Controlling the Catalytic Bond-Breaking Selectivity of Ni Surfaces by Step Blocking. *Nature Mater.* **2005**, *4*, 160−162.
(18) Picolin, A.; Busse, C.; Redinger, A.; Morgenstern, M.; Michely, T. Desorption of H_2O from Flat and Stepped Pt(111). *J. Phys. Chem. C* **2009**, *113*, 691−697.
(19) Ibach, H. Vibration Spectroscopy of Water on Stepped Gold Surfaces. *Surf. Sci.* **2010**, *604*, 377−385.
(20) van der Niet, M. J. T. C.; den Dunnen, A.; Juurlink, L. B. F.; Koper, M. T. M. The Influence of Step Geometry on the Desorption Characteristics of O_2, D_2, and H_2O from Stepped Pt Surfaces. *J. Chem. Phys.* **2010**, *132*, 174705.
(21) Arnadottir, L.; Stuve, E. M.; Jonsson, H. Adsorption of Water Monomer and Clusters on Platinum(111) Terrace and Related Steps and Kinks I. Configurations, Energies, and Hydrogen Bonding. *Surf. Sci.* **2010**, *604*, 1978−1986.
(22) Fajin, J. L. C.; Cordeiro, M. N. D. S.; Illas, F.; Gomes, J. R. B. Descriptors Controlling the Catalytic Activity of Metallic Surfaces toward Water Splitting. *J. Catal.* **2010**, *276*, 92−100.
(23) Scipioni, R.; Donadio, D.; Ghiringhelli, L. M.; Delle Site, L. Proton Wires via One-Dimensional Water Chains Adsorbed on Metallic Steps. *J. Chem. Theory Comput.* **2011**, *7*, 2681−2684.
(24) Kumagai, T.; Shiotari, A.; Okuyama, H.; Hatta, S.; Aruga, T.; Hamada, I.; Frederiksen, T.; Ueba, H. H-Atom Relay Reactions in Real Space. *Nature Mater.* **2012**, *11*, 167−172.
(25) Lin, X.; Gross, A. First-Principles Study of the Water Structure on Flat and Stepped Gold Surfaces. *Surf. Sci.* **2012**, *606*, 886−891.
(26) Donadio, D.; Ghiringhelli, L. M.; Delle Site, L. Autocatalytic and Cooperatively Stabilized Dissociation of Water on a Stepped Platinum Surface. *J. Am. Chem. Soc.* **2012**, *134*, 19217−19222.
(27) Kolb, M. J.; Calle-Vallejo, F.; Juurlink, L. B. F.; Koper, M. T. M. Density Functional Theory Study of Adsorption of H_2O, H, O, and OH on Stepped Platinum Surfaces. *J. Chem. Phys.* **2014**, *140*, 134708.
(28) Fajin, J. L. C.; Cordeiro, M. N. D. S.; Gomes, J. R. B. Density Functional Theory Study of the Water Dissociation on Platinum Surfaces: General Trends. *J. Phys. Chem. A* **2014**, *118*, 5832−5840.
(29) Greeley, J.; Jaramillo, T. F.; Bonde, J.; Chorkendorff, I.; Norskov, J. K. Computational High-Throughput Screening of Electrocatalytic Materials for Hydrogen Evolution. *Nature Mater.* **2006**, *5*, 909−913.
(30) Abild-Pedersen, F.; Greeley, J.; Studt, F.; Rossmeisl, J.; Munter, T. R.; Moses, P. G.; Skulason, E.; Bligaard, T.; Norskov, J. K. Scaling Properties of Adsorption Energies for Hydrogen-Containing Molecules on Transition-Metal Surfaces. *Phys. Rev. Lett.* **2007**, *99*, 016105.
(31) Calle-Vallejo, F.; Martinez, J. I.; Garcia-Lastra, J. M.; Rossmeisl, J.; Kooper, M. T. M. Physical and Chemical Nature of the Scaling Relations between Adsorption Energies of Atoms on Metal Surfaces. *Phys. Rev. Lett.* **2012**, *108*, 116103.
(32) Man, I. C.; Su, H.-Y.; Calle-Vallejo, F.; Hansen, H. A.; Martinez, J. I.; Inoglu, N. G.; Kitchin, J.; Jaramillo, T. F.; Norskov, J. K.; Rossmeisl, J. Universality in Oxygen Evolution Electrocatalysis on Oxide Surfaces. *ChemCatChem* **2011**, *3*, 1159−1165.
(33) Norskov, J. K.; Bligaard, T.; Rossmeisl, J.; Christensen, C. H. Towards the Computational Design of Solid Catalysts. *Nature Chem.* **2009**, *1*, 37−46.
(34) Montemore, M. M.; Medlin, J. W. Site-Specific Scaling Relations for Hydrocarbon Adsorption on Hexagonal Transition Metal Surfaces. *J. Phys. Chem. C* **2013**, *117*, 20078−20088.
(35) Vanderbilt, D. Soft Self-Consistent Pseudopotentials in a Generalized Eigenvalue Formalism. *Phys. Rev. B* **1990**, *41*, 7892−7895.
(36) Perdew, J. P.; Burke, K.; Ernzerhof, M. Generalized Gradient Approximation Made Simple. *Phys. Rev. Lett.* **1996**, *77*, 3865−3868.
(37) Monkhorst, H. J.; Pack, J. D. Special Points for Brillouin-Zone Integrations. *Phys. Rev. B* **1976**, *13*, 5188−5192.
(38) Methfessel, M.; Paxton, A. T. High-Precision Sampling for Brillouin-Zone Integration in Metals. *Phys. Rev. B* **1989**, *40*, 3616−3621.
(39) Convergence tests on Pt(221) employing plane wave cutoff up to 55 Ry and six layers confirm our results within 0.01 and 0.02 eV, respectively.
(40) Giannozzi, P.; et al. QUANTUM ESPRESSO: A Modular and Open-Source Software Project for Quantum Simulations of Materials. *J. Phys.: Condens. Matter* **2009**, *21*, 395502.
(41) Hamann, D. R. H_2O Hydrogen Bonding in Density-Functional Theory. *Phys. Rev. B* **1997**, *55*, R10157.
(42) Santra, B.; Michaelides, A.; Scheffler, M. On the Accuracy of Density-Functional Theory Exchange-Correlation Functionals for H Bonds in Small Water Clusters: Benchmarks Approaching the Complete Basis Set Limit. *J. Chem. Phys.* **2007**, *127*, 184104.
(43) Santra, B.; Michaelides, A.; Fuchs, M.; Tkatchenko, A.; Filippi, C.; Scheffler, M. On the Accuracy of Density-Functional Theory Exchange-Correlation Functionals for H Bonds in Small Water Clusters. II. The Water Hexamer and van der Waals Interactions. *J. Chem. Phys.* **2008**, *129*, 194111.
(44) Zhang, C.; Wu, J.; Galli, G.; Gygi, F. Structural and Vibrational Properties of Liquid Water from van der Waals Density Functionals. *J. Chem. Theory Comput.* **2011**, *7*, 3054−3061.
(45) Redhead, P. A. Thermal Desorption of Gases. *Vacuum* **1962**, *12*, 203−211.
(46) Sexton, B. A.; Hughes, A. E. A Comparison of Weak Molecular Adsorption of Organic Molecules on Clean Copper and Platinum Surfaces. *Surf. Sci.* **1984**, *140*, 227−248.
(47) Carrasco, J.; Klimes, J.; Michaelides, A. The Role of van der Waals Forces in Water Adsorption on Metals. *J. Chem. Phys.* **2013**, *138*, 024708.
(48) Donohue, J. *The Structure of the Elements*; Wiley, New York, 1974; p 218.
(49) Lide, D. R., Ed. *CRC Handbook of Chemistry and Physics*; CRC, New York, 2002.
(50) Grabow, L. C.; Gokhale, A. A.; Evans, S. T.; Dumesic, J. A.; Mavrikakis, M. Mechanism of the Water Gas Shift Reaction on Pt: First Principles, Experiments, and Microkinetic Modeling. *J. Phys. Chem. C* **2008**, *112*, 4608−4617.
(51) German, E. D.; Sheintuch, M. Quantum Effects in the Kinetics of H_2O Dissociative Adsorption on Pt(111), Cu(111), Rh(111), and Ni(111). *J. Phys. Chem. C* **2010**, *114*, 3089−3097.
(52) Perdew, J. P.; Ruzsinszky, A.; Csonka, G. I.; Vydrov, O. A.; Scuseria, G. E.; Constantin, L. A.; Zhou, X.; Burke, K. Restoring the Density-Gradient Expansion for Exchange in Solids and Surfaces. *Phys. Rev. Lett.* **2008**, *100*, 136406.
(53) Perdew, J. P.; Ruzsinszky, A.; Csonka, G. I.; Vydrov, O. A.; Scuseria, G. E.; Constantin, L. A.; Zhou, X.; Burke, K. Erratum: Restoring the Density-Gradient Expansion for Exchange in Solids and Surfaces. *Phys. Rev. Lett.* **2009**, *102*, 039902.
(54) Perdew, J. P.; Wang, Y. Accurate and Simple Analytic Representation of the Electron-Gas Correlation Energy. *Phys. Rev. B* **1992**, *45*, 13244.
(55) Troullier, N.; Martins, J. L. Efficient Pseudopotentials for Plane-Wave Calculations. *Phys. Rev. B* **1991**, *43*, 1993.

(56) Blöchl, P. E. Projector Augmented-Wave Method. *Phys. Rev. B* **1994**, *50*, 17953.
(57) Kresse, G.; Joubert, D. From Ultrasoft Pseudopotentials to the Projector Augmented-Wave Method. *Phys. Rev. B* **1999**, *59*, 1758.
(58) Michaelides, A.; Ranea, V. A.; de Andres, P. L.; King, D. A. General Model for Water Monomer Adsorption on Close-Packed Transition and Noble Metal Surfaces. *Phys. Rev. Lett.* **2003**, *90*, 216102.
(59) Meng, S.; Wang, E. G.; Gao, S. Water Adsorption on Metal Surfaces: A General Picture from Density Functional Theory Studies. *Phys. Rev. B* **2004**, *69*, 195404.
(60) Carrasco, J.; Michaelides, A.; Scheffler, M. Insight from First Principles into the Nature of the Bonding between Water Molecules and 4d Metal Surfaces. *J. Chem. Phys.* **2009**, *130*, 184707.
(61) Michel, C.; Göltl, F.; Sautet, P. Early Stages of Water/Hydroxyl Phase Generation at Transition Metal Surfaces—Synergetic Adsorption and O−H Bond Dissociation Assistance. *Phys. Chem. Chem. Phys.* **2012**, *14*, 15286−15290.
(62) Cao, Y.; Chen, Z.-X. Theoretical Studies on the Adsorption and Decomposition of H_2O on Pd(111) Surface. *Surf. Sci.* **2006**, *600*, 4572−4583.
(63) Pozzo, M.; Carlini, G.; Rosei, R.; Alfe, D. Comparative Study of Water Dissociation on Rh(111) and Ni(111) Studied with First Principles Calculations. *J. Chem. Phys.* **2007**, *126*, 164706.
(64) Phatak, A. A.; Nicholas Delgass, W.; Ribeiro, F. H.; Schneider, W. F. Density Functional Theory Comparison of Water Dissociation Steps on Cu, Au, Ni, Pd, and Pt. *J. Phys. Chem. C* **2009**, *113*, 7269−7276.
(65) van Grootel, P. W.; Hensen, E. J. M.; van Santen, R. A. DFT Study on H_2O Activation by Stepped and Planar Rh Surfaces. *Surf. Sci.* **2009**, *603*, 3275−3281.
(66) Smoluchowski, R. Anisotropy of the Electronic Work Function of Metals. *Phys. Rev.* **1941**, *60*, 661−674.
(67) Norskov, J. K.; Rossmeisl, J.; Logadottir, A.; Lindqvist, L.; Kitchin, J. R.; Bligaard, T.; Jonsson, H. Origin of the Overpotential for Oxygen Reduction at a Fuel-Cell Cathode. *J. Phys. Chem. B* **2004**, *108*, 17886−17892.
(68) Mavrikakis, M.; Hammer, B.; Norskov, J. K. Effect of Strain on the Reactivity of Metal Surfaces. *Phys. Rev. Lett.* **1998**, *81*, 2819−2822.
(69) Mavrikakis, M.; Rempel, J.; Greeley, J.; Hansen, L. B.; Norskov, J. K. Atomic and Molecular Adsorption on Rh(111). *J. Chem. Phys.* **2002**, *117*, 6737−6744.
(70) Krekelberg, W. P.; Greeley, J.; Mavrikakis, M. Atomic and Molecular Adsorption on Ir(111). *J. Phys. Chem. B* **2004**, *108*, 987−994.
(71) Ford, D. C.; Xu, Y.; Mavrikakis, M. Atomic and Molecular Adsorption on Pt(111). *Surf. Sci.* **2005**, *587*, 159−174.
(72) Herron, J. A.; Tonelli, S.; Mavrikakis, M. Atomic and Molecular Adsorption on Pd(111). *Surf. Sci.* **2012**, *606*, 1670−1679.
(73) The adsorption energies of OH on (221) surfaces are calculated using the same setup described in the Methods section, while adsorption energies of OH and O on (111) surfaces are taken from the literature.[68−72] We only considered the bridge site for OH adsorption which is predicted as the most stable site for Rh(221) surface.[65]